

## Effective intermediate layers for highly efficient stacked organic light-emitting devices

J. X. Sun, X. L. Zhu, H. J. Peng, M. Wong, and H. S. Kwok<sup>a)</sup>

Center for Display Research and Department of Electrical and Electronic Engineering, The Hong Kong University of Science and Technology, Clear Water Bay, Kowloon, Hong Kong

(Received 25 April 2005; accepted 7 July 2005; published online 24 August 2005)

Effective intermediate electrode layers comprising of LiF(1 nm)/Ca(25 nm)/Ag(15 nm) or LiF(1 nm)/Al(3 nm)/Au(15 nm) were studied in stacked organic light-emitting devices (OLEDs). Stacked OLEDs with two identical emissive units consisting of NPB/Alq<sub>3</sub>:C545T/BCP exhibited superior luminous efficiency-current density characteristics over conventional single-unit devices. At 20 mA/cm<sup>2</sup>, the luminous efficiency of the stacked OLEDs using the intermediate layers of LiF/Ca/Ag and LiF/Al/Au were about 19.6 cd/A and 17.5 cd/A, respectively, almost doubling that of the corresponding control devices, as expected. © 2005 American Institute of Physics. [DOI: 10.1063/1.2035320]

Stacked organic light-emitting devices (SOLEDs) with vertically stacked multiple emitting units in series were first introduced in 1996 as a means of obtaining multiple colors in a single organic light-emitting diode (OLED) device.<sup>1-3</sup> The first three-color SOLED was reported in 1997, in which the output of red, green, and blue color element can be independently controlled by adjusting the current sources.<sup>4,5</sup> Soon, SOLED was proposed as a means to obtain higher brightness and luminous efficiency.<sup>6-9</sup>

In the SOLED structure, the intermediate electrode layer connecting the adjacent emissive units plays an important role in affecting the device performance. This intermediate layer functions as an anode to one OLED unit and as a cathode for the other. Thus it can be called an anode-cathode layer (ACL). Up until now, many ACLs have been tried, such as, Mg:Ag/indium zinc oxide,<sup>6</sup> Cs:BCP/indium tin oxide (ITO),<sup>8</sup> and Cs:BCP/V<sub>2</sub>O<sub>5</sub>.<sup>9</sup> Recently, Liao *et al.*<sup>10</sup> introduced another kind of connecting unit which was comprised of Alq<sub>3</sub>:Li/NPB:FeCl<sub>3</sub> or TPBi:Li/NPB:FeCl<sub>3</sub>. As well, an intermediate layer consisting of Mg:Alq<sub>3</sub>/WO<sub>3</sub> was reported for a stacked device.<sup>11</sup> SOLEDs using ACLs mentioned above all showed very high luminous efficiency. For instance, Liao's three-unit tandem device showed a luminous efficiency of 32 cd/A based on the emission of C545T. However, in the fabrication of these ACL layers, sputtering, doping, or coevaporation of metal and organic material have to be used, which somewhat complicates the fabrication process.

In this letter, we report a new ACL which consists of LiF(1 nm)/Ca(25 nm)/Ag(15 nm) or LiF(1 nm)/Al(3 nm)/Au(15 nm). Excellent results can be obtained using these ACLs in a SOLED. The two emissive units used here are identical and consisting of NPB (4,4'-N,N'-bis[N-(1-naphthyl)-N-phenyl-amino]biphenyl)/Alq<sub>3</sub>(tris(8-hydroxy quinoline)aluminum(III)): C545T(10-(2-benzothiazolyl)-1,1,7,7-tetramethyl-2,3,6,7-tetrahydro-1H,5H,11H-benzo[1]p yrano[6,7,8-ij]quinolizin-11-one)/BCP(2,9-Dimethyl-4,7-diphenyl-1,10-phenanthroline). By employing these ACL layers, SOLEDs can be easily prepared only by thermal evaporation in vacuum chamber. The luminous efficiencies of these

SOLEDs are almost twice that of the single units, indicating good stacking. It demonstrates that these ACLs exhibit a good ability to inject electrons and holes into the bottom unit and the top one, respectively.

Four devices were studied. They are denoted as Devices A, B, C, and D with the structures of:

- (1) Device A: indium tin oxide (ITO)/NPB/Alq<sub>3</sub>:C545T/BCP/LiF/Ca/Ag/NPB/Alq<sub>3</sub>:C545T/BCP/LiF/Ca/Ag,
- (2) Device B: ITO/NPB/Alq<sub>3</sub>:C545T/BCP/LiF/Ca/Ag,
- (3) Device C: ITO/NPB/Alq<sub>3</sub>:C545T/BCP/LiF/Al/Au/NPB/Alq<sub>3</sub>:C545T/BCP/LiF/Al,
- (4) Device D: ITO/NPB/Alq<sub>3</sub>:C545T/BCP/LiF/Al.

Figure 1 shows schematic diagrams of Devices A–D, in which the thicknesses of each layer as well as the doping concentration of C545T are also shown. Although these pa-

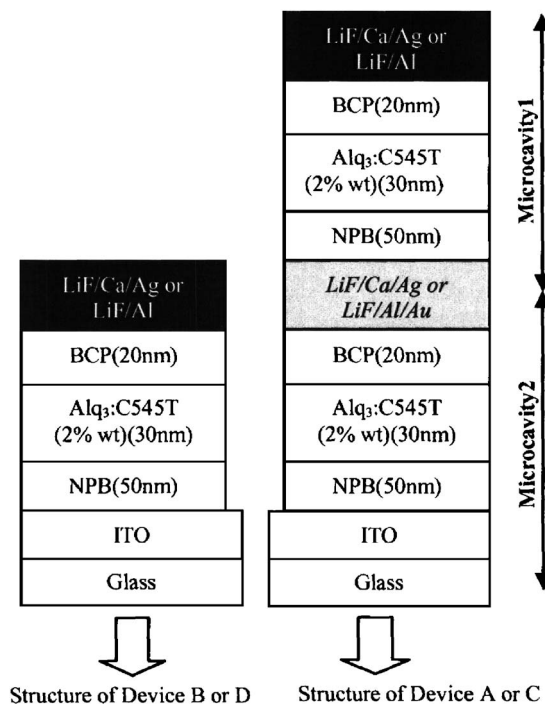


FIG. 1. Structures of Devices A–D.

<sup>a)</sup>Electronic mail: eekwok@ust.hk

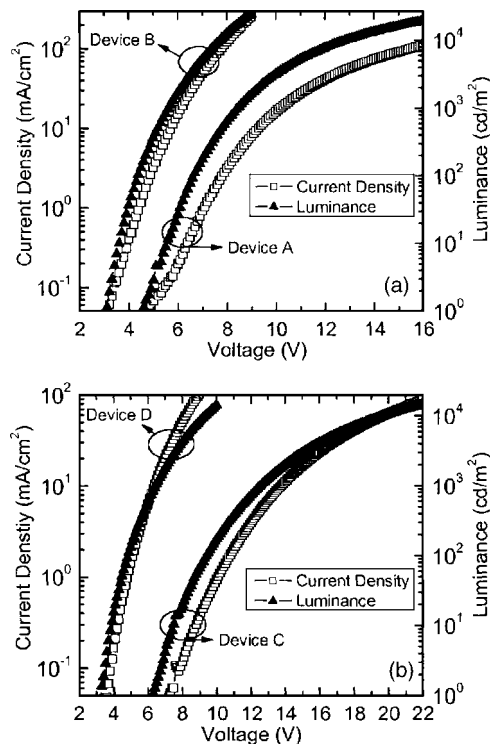


FIG. 2.  $J$ - $V$ - $L$  curves of Devices A–D: (a) Devices A and B and (b) Devices C and D.

rameters may not be the best in view of achieving highest luminous efficiency, it is enough to demonstrate the effectiveness of these new ACLs.

All the SOLEDs were fabricated on ITO-coated glass with a sheet resistance of  $\sim 25 \Omega/\text{sq}$ . The sequence of pre-cleaning the substrate consisted of soaking in ultrasonic detergent for 30 mins, spraying with de-ionized (DI) water for 10 mins, soaking in ultra-sonic-deionized water for 30 min and ovenbake dry for 1 h.<sup>12</sup>

The organic materials were commercial grade and used as received. All thin films were prepared by thermal evaporation in a four-chamber deposition system. The whole fabrication process was carried out in a vacuum chamber with a base pressure lower than  $10^{-6}$  Torr. Doping was achieved by coevaporation from two separate sources. The typical deposition rates of organic thin films and metal films were 0.1–0.2 nm/s and 0.2–0.3 nm/s, respectively. Quartz oscillators were used to monitor the film thicknesses *in situ*.

The luminance-voltage ( $L$ - $V$ ) and current density-voltage ( $J$ - $V$ ) characteristics of the SOLEDs were recorded simultaneously with a HP semiconductor parameter analyzer (model HP4145B) combined with a calibrated silicon photodiode. The electroluminescent (EL) spectra were obtained with the PR650 spectrophotometer. All measurements were

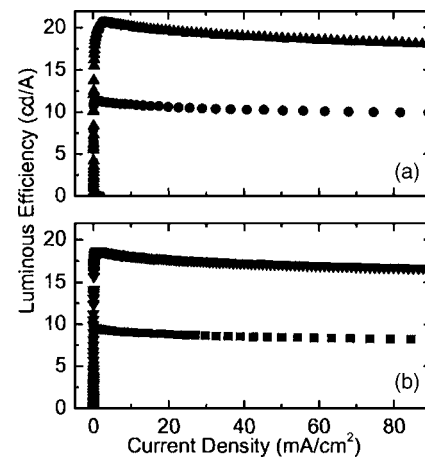


FIG. 3. Luminous efficiency vs current density curves of Devices A–D (a) Devices A (▲) and B (●); and (b) Devices C (▼) and D (■).

carried out under ambient conditions at room temperature without device encapsulation.

Figure 2 shows the  $J$ - $V$ - $L$  characteristics of Devices A–D. As expected, the driving voltages of Devices A and C are much higher than those of the control devices due to the large vertical stack structure. For example, at  $20 \text{ mA}/\text{cm}^2$ , the driving voltages of Devices A and C are about 10.4 V and 15.5 V, while those of Devices B and D are 6.1 V and 7.0 V.

Figure 3 shows the luminous efficiency versus current density curves of the devices. It is clearly seen that the luminous efficiencies of Devices A and C are about two times greater than that of single-layer Devices B and D. For example, at  $20 \text{ mA}/\text{cm}^2$ , the luminous efficiencies of Devices A, B, C, and D are 19.6 cd/A, 10.6 cd/A, 17.5 cd/A, and 8.8 cd/A, respectively. The only difference between the two control devices is the reflective cathode, which is LiF/Ca/Ag for Device B and LiF/Al for Device D. The lower work function of calcium and better reflectivity of silver contribute to the improvement of luminous efficiency of Device B compared to Device D with the conventional bilayer cathode LiF/Al.

The doubled efficiency of Devices A and C, with respect to those corresponding control devices, is attributed to the high efficiency of the ACLs which can generate electrons on one side and holes on the other side. Both light emissive units can efficiently produce light under the same current driving. It can also be seen that although higher driving voltages are needed in SOLEDs, the power efficiency is similar to the single-emissive unit device due to the higher luminous efficiencies. Table I summarizes the key EL characteristics of the studied devices.

Figure 4 shows the EL spectra of Devices A and B in the normal direction. The EL spectra of Devices A and B both

TABLE I. The Key EL characteristics of Devices A–D.

Samples	Turn-on voltage (with $1 \text{ cd}/\text{m}^2$ )	Voltage required for $20 \text{ mA}/\text{cm}^2$	Power efficiency @ $100 \text{ cd}/\text{m}^2$	Power efficiency @ $1000 \text{ cd}/\text{m}^2$	Power efficiency @ $10\,000 \text{ cd}/\text{m}^2$
Device A	4.6 V	10.4 V	8.8 lm/W	7.61 lm/W	4.56 lm/W
Device B	3.0 V	6.1 V	8.18 lm/W	6.17 lm/W	4.03 lm/W
Device C	6.3 V	15.5 V	6.15 lm/W	4.61 lm/W	2.72 lm/W
Device D	3.3 V	7 V	6.12 lm/W	4.38 lm/W	2.67 lm/W

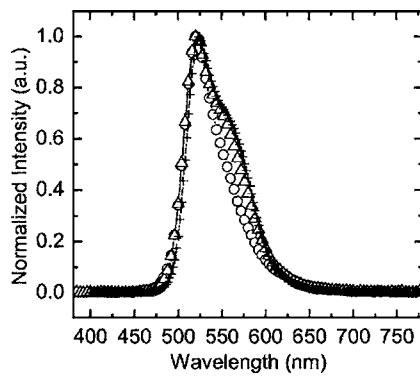


FIG. 4. EL spectra of Devices A (Measured:  $\Delta$  Calculated:  $+$ ) and B:  $\circ$ ).

peak at 520 nm except that the full width of half maximum of the former ( $\sim 66$  nm) is larger than that of the latter ( $\sim 52$  nm). This is the result of microcavity effects in Device A. Due to the semitransparency of the ACL, two microcavities are formed within Device A. Figure 5 is a plot of the spectra of Device A at different viewing angles. It can be seen that there is a small deviation between the spectra at different viewing angles further indicating the existence of microcavity effect.<sup>13</sup>

We also calculated the emission spectra of the stacked device. As an example, the calculated spectrum of Device A in the normal direction is shown in Fig. 4. The calculation is based on the model given in Refs. 14 and 15. Details can be found in our previous paper (see Ref. 16). Here, we used the measured EL spectra in the normal direction of Device B as the intrinsic radiation spectrum of the C545T emitter. It was then used to calculate the spectrum of the bottom and top emissive units of Device A, with microcavity taken into account. Then, the output spectrum of Device A is taken as the sum of these two individual spectra, with the assumption of: (i) The ACL combined with the top emissive unit and top cathode behaves as a single reflective mirror for bottom device; and (ii) ITO anode capped with the bottom emissive unit and the ACL is treated as a single semitransparent mirror for top device. The reflectance and transmittance were calculated using the transfer-matrix method.<sup>17</sup> The calculated

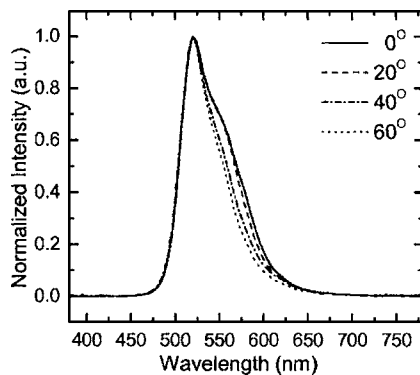


FIG. 5. The measured EL spectra of Device A at different viewing angles.

spectrum agrees well with the measured one (see Fig. 4). It is believed that better EL performance of the stacked OLED can be easily achieved by optimizing thickness through a more careful optical simulation.<sup>13</sup> This calculation, including the microcavity effect, can be used to optimize the thicknesses of the many layers in the stacked device.

In summary, two-unit stacked OLEDs utilizing new ACLs have been fabricated. The doubled luminous efficiency under the same current density compared to the conventional single-unit device demonstrates that the ACL can effectively function as the connecting unit between OLED layers. It is believed that the optimization in performance can further be achieved through a careful optical simulation of the microcavity effect. Interestingly, the stacked OLEDs using the ACLs can not only operate in the constant current mode but can also be operated in the individual control mode. Thus, each organic emissive unit can be individually controlled to yield different color emissions.<sup>4</sup> We also have preliminary results showing that the color can be controlled by the voltage on the stacked device.

This research was supported by the Innovations and Technology Fund of the Hong Kong SAR government.

<sup>1</sup>V. Bulovic, G. Gu, P. E. Burrows, M. E. Thompson, and S. R. Forrest, *Nature (London)* **380**, 29 (1996).

<sup>2</sup>G. Gu, P. E. Burrows, S. R. Forrest, and M. E. Thompson, *Appl. Phys. Lett.* **68**, 2606 (1996).

<sup>3</sup>P. E. Burrows, S. R. Forrest, S. P. Sibley, and M. E. Thompson, *Appl. Phys. Lett.* **69**, 2959 (1996).

<sup>4</sup>Z. Shen, P. E. Burrows, V. Bulovic, S. R. Forrest, and M. E. Thompson, *Science* **276**, 2009 (1997).

<sup>5</sup>P. E. Burrows, G. Gu, V. Bulovic, Z. Shen, S. R. Forrest, and M. E. Thompson, *IEEE Trans. Electron Devices* **44**, 1188 (1997).

<sup>6</sup>S. Tanaka and C. Hosakawa, U.S. Patent No. 6,107,734 (22 August 2000).

<sup>7</sup>G. W. Jones and W. E. Howard, U.S. Patent No. 6,337,492 B1 (8 January 2002).

<sup>8</sup>J. Kido, T. Nakada, J. Endo, N. Kawamura, K. Mori, A. Yokoi, and T. Matsumoto, *Proceedings 11th International Workshop on Inorganic and Organic Electroluminescence and 2002 International Conference on the Science and Technology of Emissive Displays and Lighting*, Ghent, Belgium, 23–26 September 2002 (Universiteit Gent, Ghent, Belgium, 2002), p. 539.

<sup>9</sup>T. Matsumoto, T. Nakada, J. Endo, K. Mori, N. Kawamura, A. Yokoi, and J. Kido, *SID 03 Digest* **34**, 979 (2003).

<sup>10</sup>L. S. Liao, K. P. Klubek, and C. W. Tang, *Appl. Phys. Lett.* **84**, 167 (2004).

<sup>11</sup>C.-C. Chang, S.-W. Hwang, C. H. Chen, and J.-F. Chen, *Jpn. J. Appl. Phys., Part 1* **43**, 6418 (2004).

<sup>12</sup>J. X. Sun, X. L. Zhu, H. J. Peng, M. Wong, and H. S. Kwok, *SID Symposium Digest* **36**, 797 (2005).

<sup>13</sup>V. Bulovic, V. B. Khalfin, G. Gu, P. E. Burrows, D. Z. Garbuzov, and S. R. Forrest, *Phys. Rev. B* **58**, 3730 (1998).

<sup>14</sup>H. Benisty, H. De Neve, and C. Weisbuch, *IEEE J. Quantum Electron.* **34**, 1612 (1998).

<sup>15</sup>K. Neyts, P. de Visschere, D. K. Fork, and G. B. Anderson, *J. Opt. Soc. Am. B* **17**, 114 (2000).

<sup>16</sup>C. Qiu, H. Peng, H. Chen, Z. Xie, M. Wong, and H. S. Kwok, *IEEE Trans. Electron Devices* **51**, 1207 (2004).

<sup>17</sup>M. Born and E. Wolf, *Principles of Optics*, 7th ed. (Cambridge University Press, Cambridge, UK, 1999).